High-energy polarization in exclusive reactions at large angles

P. Chiappetta and J. Soffer
Centre de Physique Théorique, Centre National de la Recherche Scientifique, Luminy, Case 907, F-13288 Marseille Cedex 9, France
(Received 2 March 1983)

We analyze several interesting high-energy two-body reactions at large angles in the framework of the massive-quark model. We propose to use spin-dependent effects to test the validity of this model and to compare it with different theoretical approaches for describing hadronic interactions at short distances.

I. INTRODUCTION

Large-angle two-body processes at high energies are considered a most important class of reactions to test our understanding of the deep structure of hadrons. The scattering amplitudes which describe the dynamics in this particular kinematic region depend on the interactions of the hadronic constituents at short distances and on large-momentum behavior of the hadronic form factors, which is believed to contain basic information about the composite nature of hadrons. Experimental tests are needed to define precisely the limits of validity of any serious theoretical proposal on this question. In what follows we will see that the differential cross sections are indeed important to measure, but polarizations are even more so, because they can uncover very fundamental aspects of the underlying quark dynamics. The striking spin correlation in pp elastic scattering near $\theta_{\text{c.m.}}=90°$ measured at Argonne with a polarized proton beam of 11.75 GeV/c (Ref. 1) has inspired a fairly large number of theoretical papers.[2–8] For massless quarks the QCD vector interaction preserves the quark helicity and this strong spin constraint leads to a selection rule for hadron helicities,

$$\lambda_a+\lambda_b=\lambda_{a'}+\lambda_{b'}\ , \tag{1}$$

for the reaction $a+b\to a'+b'$. This important property has several interesting consequences,[9] and, in particular, all single-spin asymmetries are expected to vanish near $\theta_{\text{c.m.}}=90°$. The situation is rather distinct in the case of a theoretical approach of short-distance phenomena based on the massive-quark model (MQM), which gave a satisfactory description of recent data on large-angle baryon-baryon and meson-baryon elastic scattering.[4,10] The aim of this work is to reexamine some specific features of this approach and to present new predictions from it. The outline of the paper is as follows. In the next section we briefly review the method we use to build up helicity amplitudes for two-body reactions. In Sec. III we discuss several baryon-baryon reactions and, in particular, $\bar{p}p$ elastic scattering, together with some recent data from CERN.[11] Section IV is devoted to meson-baryon scattering where important polarization effects are predicted. We make a comparison between various theoretical models in Sec. V, where we will give our concluding remarks.

II. LARGE-ANGLE HELICITY SCATTERING AMPLITUDES

Although the basic ideas of the MQM (Ref. 12) contain some obvious features of hadron interactions, it was necessary to make it more realistic by using the bag idea to describe hadrons as confined in space-time regions where quarks move almost freely. In quark geometrodynamics[13] (QGD) confinement is introduced geometrically, i.e., one requires the wave function to vanish outside a compact space-time region. The physical hadronic states correspond to a limited number of "allowed orbits" where quarks can only propagate. This constraint leads to a solution for the baryon spectrum,[14] in which the three quarks are spatially aligned, equivalent to a quark-diquark structure. Such a suppression of dynamical degrees of freedom avoids the supermultiplets (70, 0^+) and (20, 1^+), unobserved so far in the mass region below 2 GeV, but which are present in the MQM and in various other quark models. The transitions between the physical states are essentially given by the space-time overlap which is indeed relevant to calculating decay processes and scattering reactions. In order to evaluate the large angle helicity amplitudes for the reaction $a+b\to a'+b'$ at high energies, we must consider the basic diagram Fig. 1(a) and, perhaps,

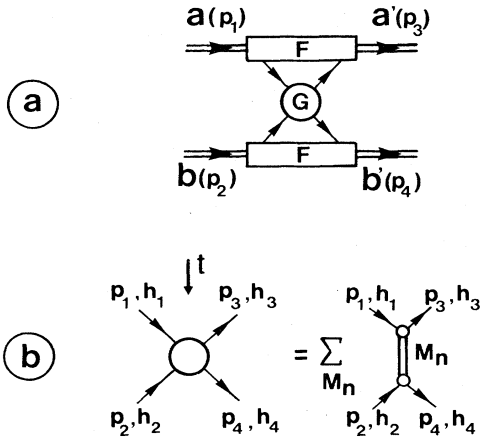

FIG. 1. (a) The basic MQM diagram describing the large-angle reaction $a+b\to a'+b'$. (b) the $qq\to qq$ amplitude in QGD.

some symmetric partner depending on what reaction we are looking at. They are obtained by folding the hadron overlap functions $F(aa';qq')$ and $F(bb';qq')$, appearing in the upper and lower parts of the diagram, with the elementary quark-quark (or quark-antiquark) amplitude at large angles. In the hadron overlap functions we must specify, on the one hand, the spin and flavor structure which we take from the simple SU(6) hadron wave functions and, on the other hand, the energy dependence which must recover, in the high-energy limit, the observed behavior of the hadron form factors. Here let us stress that we are using a spin-conserving overlap, that is, we assume spin conservation (not helicity conservation) for the spectator quarks—which is a natural assumption. The hadron overlap functions are expressed in terms of θ, the center-of-mass angle between the two hadrons a and a' (or b and b'), and E, the center-of-mass energy of the active quark. Their general expressions for baryons and mesons were explicitly given in Refs. 4 and 10 and they will be recalled below in a suitable form for practical calculations. For the quark-quark (or quark-antiquark) amplitude G which appears in the middle of the diagram 1(a), we must also distinguish its spin structure from its energy dependence. According to QGD, G is given by the sum of an infinite number of mesons [see Fig. 1(b)] belonging to four different meson families [transverse vector (V_T), pseudoscalar (P), and longitudinal vector (V_L)], which are the four different spin configurations of the $q\bar{q}$ system. This rich spin structure gives, asymptotically,

$$G_{h_1h_2,h_3h_4}(\theta,E)=4E^2\sum_{i=0}^{3}\alpha_i(\sigma_i)_{h_4h_2}(\sigma_i)_{h_3h_1} \tag{2}$$

with

$$\alpha_0=\frac{3+\cos\theta}{2},\quad \alpha_1=\alpha_3=\frac{1-\cos\theta}{2},\quad \alpha_2=\langle s\rangle\left[\frac{1-\cos\theta}{2}\right]. \tag{3}$$

The h_i ($i=1,\ldots,4$) denote the quark helicities. The (V_T) are related to α_0 and α_3, the (P) to α_1, and the (V_L) to α_2, as can be easily checked. The coefficient $\langle s\rangle$ occurring in α_2 is an important factor because it is the relative weight of longitudinal to transverse. In QGD it is basically related to the mass of the external hadrons and it will have different values in different reactions and according to the large-angle diagram we will consider. For example, in the case of $a+b\to a'+b'$ for the diagrams given in Fig. 1, we find

$$\langle s\rangle=\frac{R^2}{\pi}(m_a+m_{a'})(m_b+m_{b'}) \tag{4}$$

with $R^2\simeq 2\ \mathrm{GeV}^{-2}$ from the slope of the Regge trajectories. To obtain the full amplitude G we ought to multiply $G_{h_1h_2,h_3h_4}$ by $G(t,u)$, the explicit sum over all meson resonances which occur in the t channel of diagram 1(b). We have

$$G(t,u)=\sum_n\frac{1}{m_n^2}\frac{1}{m_n^2-t}\sum_{l=0}^{l_{\max}}(2l+1)P_l\left[1+\frac{2u}{m_n^2}\right], \tag{5}$$

and it is clear that since we look at a qq amplitude, the Regge behavior occurs in the u channel. For our purpose we must evaluate the limit of $G(t,u)$ for t and u large, and according to the techniques developed in Ref. 15 we find

$$G(t,u)\to\ln(-t/m_0^2)\frac{1}{(-u)^{3/2}}. \tag{6}$$

This ends our discussion of the qq amplitude G which applies to Fig. 1(b), but clearly for other configurations and $q\bar{q}$ amplitudes[10] the spin-dependent part of G has basically the form of Eq. (2) with the appropriate helicity labels and different coefficients α_i. Its energy dependence comes essentially from Eq. (6) by setting different limits. The high-energy dependence of the hadron overlap functions F is such that it must lead to the observed asymptotic behavior of the corresponding hadron form factors.

In the folding of FGF which must be done to construct the helicity amplitudes, it is useful to perform the sum over the quark helicities. Apart from some factors related to the energy dependence of F and G, the helicity amplitudes are

$$\phi_{\{\lambda\}}\sim\sum_{i=0}^{3}\alpha_i\sum_{\{q\}}\tilde{F}^{(i)}_{\lambda_a\lambda_{a'};q_aq_{a'}}(\theta)\tilde{G}_{q_aq_{a'};q_bq_{b'}}\tilde{F}^{(i)}_{\lambda_b\lambda_{b'};q_bq_{b'}}(\theta). \tag{7}$$

(For the definition of the helicity amplitudes and complete expression of the various observables for $a+b\to a'+b'$, see Ref. 16.) The nature of the sum over the q's which denote quark internal degrees of freedom depend on the configuration considered corresponding to a specific expression of $\tilde{G}$, and the $\tilde{F}^{(i)}$ have the following explicit forms. If a (a') is a spin—one-half baryon we obtain

$$\begin{aligned}
\tilde{F}^{(0)}_{\lambda\lambda';qq'}&=\delta_{\lambda\lambda'}[A_q^{q'}(4-\cos\theta)+S_q^{q'}(1+2\cos\theta)]+\epsilon_{\lambda\lambda'}\sin\theta(2S-A)_q^{q'},\\
\tilde{F}^{(1)}_{\lambda\lambda';qq'}&=(\sigma_1)_{\lambda'\lambda}(5A-S)_q^{q'},\\
\tilde{F}^{(2)}_{\lambda\lambda';qq'}&=(\sigma_2)_{\lambda'\lambda}[A_q^{q'}(4+\cos\theta)+S_q^{q'}(1-2\cos\theta)]+i\delta_{\lambda\lambda'}\sin\theta(2S-A)_q^{q'},\\
\tilde{F}^{(3)}_{\lambda\lambda';qq'}&=(\sigma_3)_{\lambda'\lambda}(5A-S)_q^{q'}
\end{aligned} \tag{8}$$

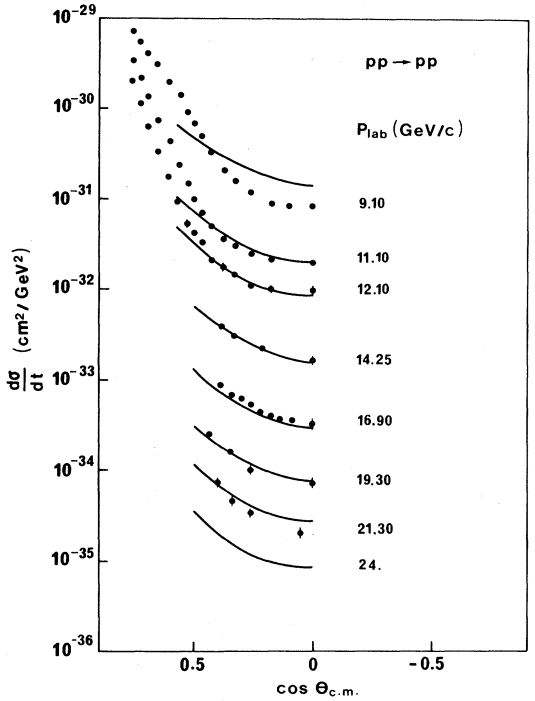

FIG. 2. Comparison of our predictions normalized at 90° for $p_{\text{lab}}=11.10$ GeV/c with the experimental results of Ref. 17.

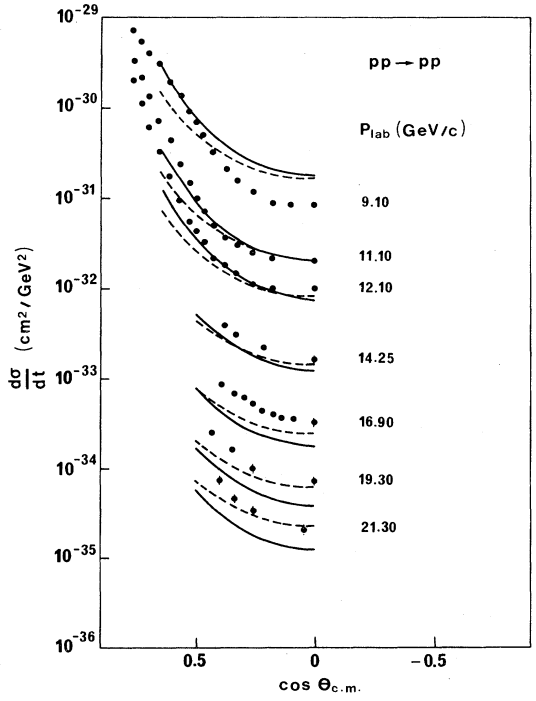

FIG. 3. Comparison of the predictions of the CIM models, Ref. 18 (solid curve) and Ref. 19 (dashed curve), with the data of Ref. 17. The normalization is the same as in Fig. 2.

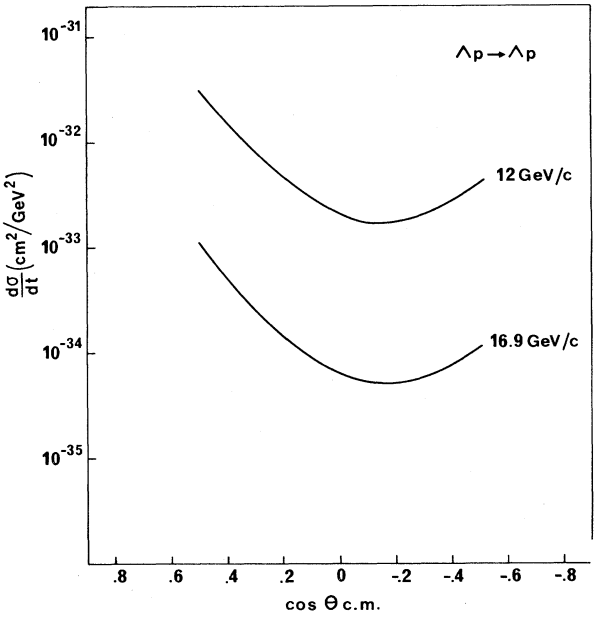

FIG. 4. Absolute predictions of our model for $\Lambda p \to \Lambda p$.

with

$$A_q^{q'}=(A_{aa'})_q^{q'}=(B_a\bar{B}_{a'})_q^{q'}\ ,$$
$$S_q^{q'}=(S_{aa'})_q^{q'}=\delta_q^{q'}\mathrm{Tr}(\bar{B}_aB_{a'})-(\bar{B}_{a'}B_a)_q^{q'}\ , \tag{9}$$

where B_a is the SU(3) matrix of a. If a (a') is a pseudoscalar meson we obtain

$$\tilde{F}_{qq'}^{(0)}=2\cos(\theta/2)m_q^{q'}\ ,$$
$$\tilde{F}_{qq'}^{(1)}=\tilde{F}_{qq'}^{(3)}=0\ , \tag{10}$$
$$\tilde{F}_{qq'}^{(2)}=2i\sin(\theta/2)m_q^{q'}\ ,$$

with

$$m_q^{q'}=(m_{aa'})_q^{q'}=(M_aM_{a'}^{\dagger})_q^{q'}\ ,$$

where M_a is the SU(3) matrix of a.

These are the essential steps one needs to derive the helicity amplitudes for the different reactions we will study in the following sections.

III. BARYON-BARYON SCATTERING

Let us start with pp elastic scattering which has been extensively measured in the large angle region. In Ref. 4 the five amplitudes were calculated, but the main point was to show that this approach leads to a fairly good description of the data on the spin correlation parameters. Here we will simply complete the comparison of the model with the available data on the differential cross section.[17] This is done in Fig. 2 at various energies. Above $p_{\text{lab}}=10$ GeV/c both the energy behavior and the angular dependence are in fair agreement with the data. We have also made the comparison with the constituent-interchange model (CIM) where quarks are simply interchanged in the scattering process. Two different versions of this model[18,19] are shown in Fig. 3 and they fail to reproduce the data. Below 10 GeV/c, one does not expect any of

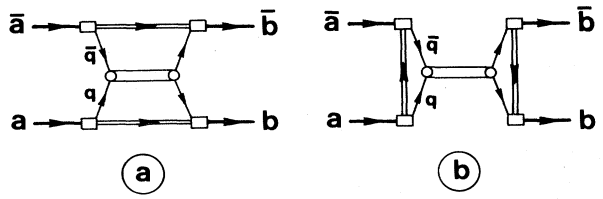

FIG. 5. The two basic MQM diagrams describing the large angle reaction $a+\bar{a}\to b+\bar{b}$.

these models to be highly reliable.

We can predict easily other baryon-baryon elastic cross sections by using the appropriate flavor dependence in Eq. (8) with no additional parameter; in particular, the normalization is now fixed. As an example we show in Fig. 4 our absolute predictions for $\Lambda p\to\Lambda p$ at two different energies, which should be checked experimentally. The cross section is below that of $pp\to pp$ and clearly not symmetric around 90°.

Let us now discuss a class of baryon-antibaryon reactions, that is, $a+\bar{a}\to b+\bar{b}$, which will be applied in particular to the scattering $\bar{p}p\to\bar{p}p$. In this case the two relevant diagrams are presented in Fig. 5. They both involve $q\bar{q}$ scattering, but whereas Fig. 5(a) requires, from the flavor sum [Eq. (8)], the product of the traces $\mathrm{Tr}\tilde{F}\times\mathrm{Tr}\tilde{F}$, for Fig. 5(b) we have the trace of the product with both $\tilde{F}(\theta)$ evaluated at $\theta=\pi$. This last diagram which corresponds to the annihilation into true meson resonances gives rise to a phase through the factor occurring in Eq. (6); that is,

$$\ln(-s/m_0^2)=\ln(s/m_0^2)-i\pi\ . \tag{11}$$

The helicity amplitudes, incompletely defined as in Eq. (7), corresponding to the graph 5(a) are

$$\begin{aligned}
&\phi_1\sim(2+\cos\theta)^2\alpha_0-\sin^2\theta\alpha_2+\alpha_3\ ,\\
&\phi_2\sim(2+\cos\theta)^2\alpha_0+\sin^2\theta\alpha_2-\alpha_3\ ,\\
&\phi_3\sim\sin^2\theta\alpha_0+\alpha_1-(2-\cos\theta)^2\alpha_2\ ,\\
&\phi_4\sim-\sin^2\theta\alpha_0+\alpha_1+(2+\cos\theta)^2\alpha_2\ ,\\
&\phi_5\sim-3\sin\theta[(2+\cos\theta)\alpha_0-(2-\cos\theta)\alpha_2]\ ,\\
&\phi_6=-\phi_5
\end{aligned} \tag{12}$$

with

$$\alpha_0=\frac{1-\cos\theta}{2}\ ,\quad \alpha_1=\alpha_3=\frac{3\cos\theta-1}{2}\ ,\quad \alpha_2=\tfrac{1}{2}\ . \tag{13}$$

Note that although we expect six different amplitudes, the model reduces to the situation of identical particles.

Similarly, the set of amplitudes corresponding to the graph 5(b) is

$$\begin{aligned}
&\bar{\phi}_1\sim 17(\bar{\alpha}_0+\bar{\alpha}_3),\ \bar{\phi}_2\sim 17(\bar{\alpha}_0-\bar{\alpha}_3)\ ,\\
&\bar{\phi}_3\sim 17\bar{\alpha}_1-45\bar{\alpha}_2\ ,\ \bar{\phi}_4\sim 17\bar{\alpha}_1+45\bar{\alpha}_2\ ,\\
&\bar{\phi}_5=\bar{\phi}_6=0
\end{aligned} \tag{14}$$

with

$$\bar{\alpha}_0=\frac{1+\cos\theta}{2}\ ,\quad \bar{\alpha}_1=\bar{\alpha}_2=\frac{1-\cos\theta}{2}\ ,\quad \bar{\alpha}_3=1-\cos\theta\ . \tag{15}$$

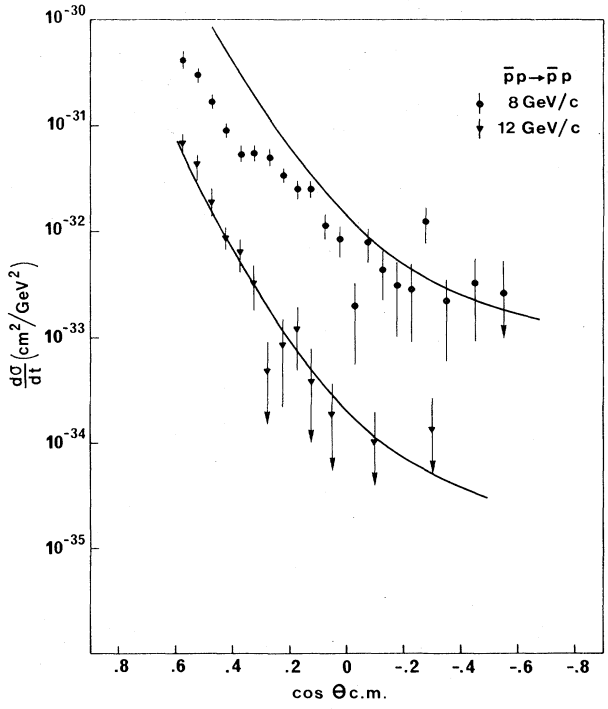

FIG. 6. Comparison of our absolute predictions with the experimental results of Ref. 11.

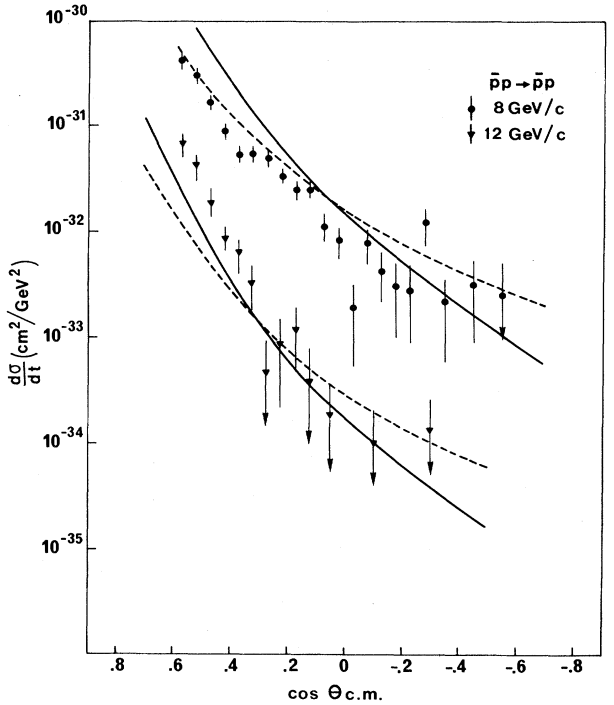

FIG. 7. Comparison of the predictions of the CIM models, Ref. 18 (solid curve) and Ref. 19 (dashed curve), with the data of Ref. 11.

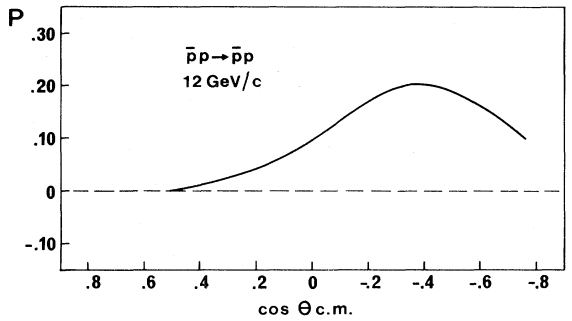

FIG. 8. The predicted polarization for $\bar{p}p \to \bar{p}p$ from our model.

In Fig. 6 we give the comparison of our predictions for the differential cross section for $\bar{p}p \to \bar{p}p$ with recent CERN data.[11] A reasonable agreement is obtained at $p_{\text{lab}} = 12$ GeV/c for both the angular dependence and the ratio $r = pp/\bar{p}p$ at 90°, which is roughly 20. As for $pp \to pp$, the curve is too high at $p_{\text{lab}} = 8$ GeV/c. In Fig. 7 we compare the same data with the two CIM versions considered above.[18,19] The model of Ref. 18 suggests

$$r \sim \left[\frac{2}{1+\cos\theta} \right]^{5.6} , \tag{16}$$

whereas that of Ref. 19 predicts

$$r = \frac{16}{(1+\cos\theta)^4} . \tag{17}$$

The last angular dependence appears to be too flat to be in agreement with the 12 GeV/c data.

In addition, for these two models all the amplitudes produced are real and therefore one does not expect any polarization. This contrasts with our model, which produces two sets of amplitudes with different phases [see Eq. (11)]. As a result, we have a nonzero polarization P which is presented in Fig. 8. The prediction is given at 12 GeV/c, which is accessible to experiment, but it is almost energy independent.

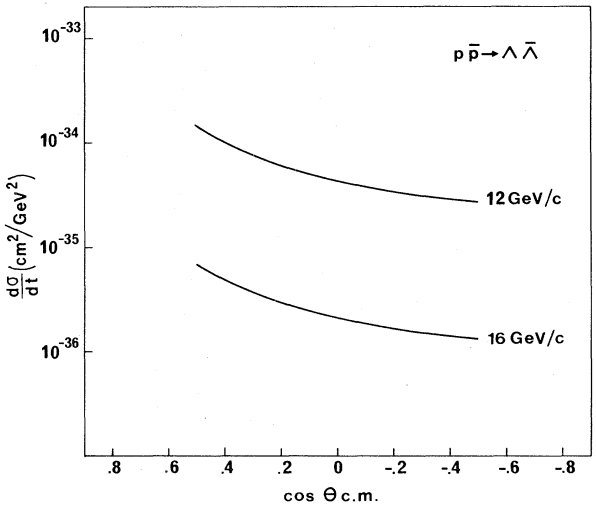

FIG. 9. Our absolute predictions for $p\bar{p} \to \Lambda\bar{\Lambda}$.

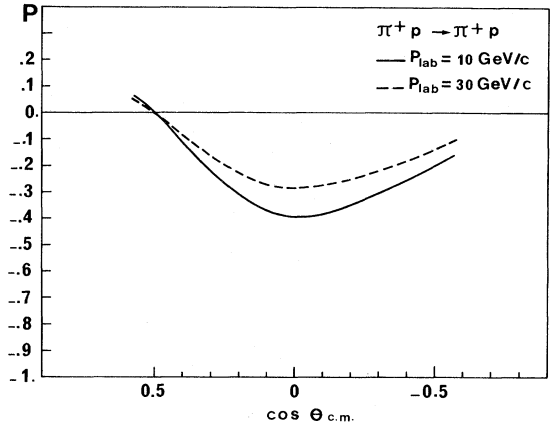

FIG. 10. Our predicted polarization for $\pi^+ p \to \pi^+ p$.

We have also studied the reaction $\bar{p}p \to \bar{\Lambda}\Lambda$. In this case only the diagram of Fig. 5(b) contributes. As a consequence we expect no polarization. Absolute predictions for the differential cross sections, which should be checked experimentally, are given in Fig. 9.

IV. MESON-BARYON SCATTERING

Meson-baryon elastic scattering also has been recently analyzed in the framework of the MQM.[10] For this type of reaction, two classes of diagrams contribute: the meson exchange and the baryon exchange graphs. The relative normalization between these two contributions is an unknown parameter λ which must be determined from data. Both energy and angular dependences of the differential cross section were shown to be in good agreement with recent CERN data on $\pi^{\pm}p$ scattering[20] for $\lambda = -\frac{1}{20}$. This value was determined from $\pi^+ p$ elastic scattering at 10 GeV/c.[21] Another value of λ was proposed later from the fit of the $\pi^- p$ differential cross section[22] where they found $\lambda = +\frac{1}{10}$. Present data are not accurate enough to allow a definite choice.

Let us now turn to the polarization. A phase difference giving rise to a nonzero polarization occurs only when one

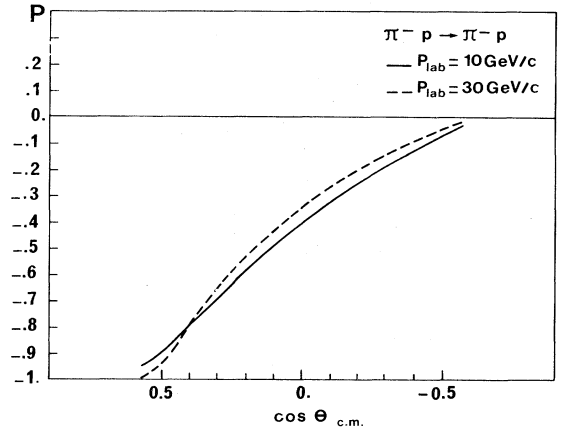

FIG. 11. Our predicted polarization for $\pi^- p \to \pi^- p$.

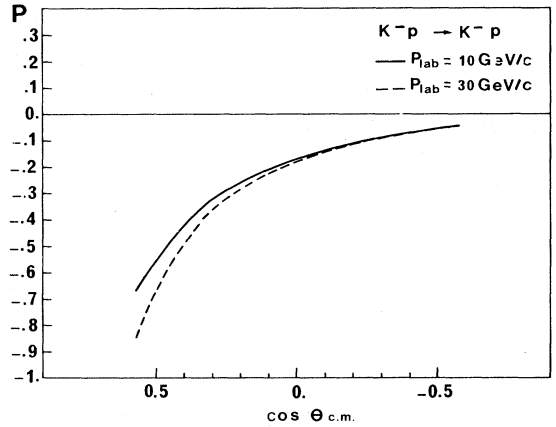

FIG. 12. Our predicted polarization for $K^-p \to K^-p$.

of the diagrams involved in a given reaction corresponds to the production of true resonances in the s channel. In order to get a large polarization the contribution corresponding to this diagram must interfere with another large contribution. This is the case for the elastic reactions $\pi^{\pm}p$ and K^-p but we expect no polarization for K^+p, which is an exotic reaction in the s channel. For $\pi^-p \to K^0\Lambda$ we certainly have true resonances in the s channel, but in this model it must interfere with the meson exchange diagrams which are suppressed due to the small value of λ. Keeping $\lambda = -\frac{1}{20}$ we give in Figs. 10—12 the polarizations P for the reactions $\pi^{\pm}p$ and K^-p. Contrary to QCD which predicts no polarization in all cases, the polarizations at 90° are about -40% for $\pi^{\pm}p$ and -20% for K^-p. The predictions are quite independent of the incident energy but they strongly depend on the parameter λ. If we take instead $\lambda = +\frac{1}{10}$ we also obtain large polarizations but different shapes. So our predictions can only be considered as a guideline rather than a definite test of the model. Of course, if λ is known unambiguously, using, for example, one polarization measurement, then the predictions for the other reactions will become absolute.

V. COMPARISON BETWEEN THE THEORETICAL MODELS AND CONCLUDING REMARKS

Our aim in this section is to compare the predictions of the CIM and the MQM in the cases of both the differential cross section and the spin-dependent observables. All these quantities depend on the incident energy and on the scattering angle.

Let us first discuss the energy dependence of the cross section. In the CIM-type models the power behavior in s can be obtained from a counting rule based on dimensional arguments.[23] This leads to the behavior s^{-10} for baryon-baryon scattering and s^{-8} for meson-baryon scattering. The CIM can be reinterpreted in the framework of perturbative QCD. The gluonic exchange between the constituents of the same hadron leads to a violation of the counting rule. The energy behavior is affected by logarithmic corrections.[24] Moreover, the absolute normalization should now be fixed by summing all the diagrams, but this is a huge task. The energy dependence of the differential cross section is somehow different in the MQM. The logarithmic term [see Eq. (6)] in the quark-quark and quark-antiquark amplitudes induces a dependence like $s^{-11}\ln^2(s/m_0^2)$ for baryon-baryon scattering and $s^{-9}\ln^2(s/m_0^2)$ for meson-baryon scattering. We should not forget, in the QCD framework, the Landshoff[25] contributions arising from three successive nearly on-shell quark-quark diffusions in baryon-baryon scattering. The differential cross section is proportional to s^{-8} at fixed angle. This slow falloff with energy has not yet been clearly observed. However, Sudakov form factors arising from quark-quark-gluon vertices tend to restore the behavior given by the counting rule[26] and provide a possible interpretation of the observed oscillations of the elastic proton-proton cross section with $\ln s$.[27] Unfortunately, the currently available high-energy data are not accurate enough to clearly discriminate between the counting rule, and QCD logarithmic corrections, and the MQM prediction.

The situation is the same for the angular distribution of the differential cross section but not for the spin-dependent parameters. When the kinematical invariants s, t, and u are large compared to the quark masses, the quarks can be taken as massless. In this case their coupling to vector gluons conserves helicity. This leads to important consequences. First of all, any polarization proportional to a spin-flip amplitude is zero. This is the case of all transverse polarization involving one spin. For proton-proton scattering the two double-spin asymmetries A_{NN} and A_{LL} are related[16] at $\theta_{\text{c.m.}} = 90°$ by

$$2A_{NN} - A_{LL} = 1 \ . \tag{18}$$

This strong rule has not yet been really tested. Indeed at $p_{\text{lab}} = 11.75$ GeV/c A_{NN} is well known, but the determination of A_{LL} at the same energy is still preliminary.[28] Moreover, in the absence of phase differences (this situation might not occur in the presence of imaginary parts coming from Sudakov corrections) the helicity conservation leads to the following relations for the spin-correlation parameter[29]:

$$\left|\begin{matrix} D_{NN} \\ K_{NN} \end{matrix}\right| = \{\tfrac{1}{2}(1-A_{LL})(1+A_{LL}) \pm [(1+A_{LL})^2 - 4A_{NN}^2]^{1/2}\}^{1/2} . \tag{19}$$

This relation has some ambiguity because the relative sign in the right-hand side of Eq. (19) is related either to D_{NN} or K_{NN}, and only when one is determined is the other one fixed. So measurements at the same energy of all double-spin asymmetries are needed to confirm in a definite way this helicity selection rule. A comment is in order here. A violation of this rule would indicate the presence of other mechanisms like wave-functions effects[5,8] in the connection between quark and nucleon amplitudes or higher-twist terms.

The situation is rather different in the case of our theoretical approach based on massive quarks where the elementary qq and $q\bar{q}$ amplitudes involve vector, scalar, and pseudoscalar couplings. The spin-correlation parameters have been already calculated, and Eqs. (18) and (19)

do not hold. For a given reaction several diagrams can contribute and the polarization is nonzero if one of them corresponds to the production of true resonances in the s channel. This is the case for $\bar{p}p$, $\pi^{\pm}p$, and $K^{-}p$ elastic scattering. We recall here the sensitivity to the parameter λ of the predictions for meson-baryon scattering. Therefore, polarization data at large angles are important tools to discriminate between challenging models.

ACKNOWLEDGMENTS

We are grateful to G. Preparata for several interesting discussions at various stages of this work. One of us (P.C.) would like to thank the Commissariat A. L'Energie Atomique for financial support.

[1]P. G. Crabb *et al.*, Phys. Rev. Lett. 41, 1257 (1978); J. R. O'Fallon *et al., ibid.*, 39, 733 (1977).
[2]G. Farrar, S. Gottlieb, D. Sivers, and G. M. Thomas, Phys. Rev. D 20, 202 (1979).
[3]S. J. Brodsky, C. E. Carlson, and H. Lipkin, Phys. Rev. D 20, 2278 (1979).
[4]G. Preparata and J. Soffer, Phys. Lett. 86B, 304 (1979).
[5]J. Szwed, Phys. Lett. 93B, 485 (1980).
[6]G. F. Wolters, Phys. Rev. Lett. 45, 776 (1980).
[7]C. Avilez, G. Cocho, and M. Moreno, Phys. Rev. D 24, 634 (1981).
[8]M. Anselmino, Z. Phys. C 13, 63 (1982).
[9]S. J. Brodsky and G. P. Lepage, Phys. Rev. D 24, 2848 (1981).
[10]G. Preparata and J. Soffer, Phys. Lett. 93B, 187 (1980).
[11]Data from the WA 13 experiment (CERN—College de France—Neuchatel collaboration), A. De Bellefon *et al.*, CERN report (unpublished).
[12]G. Preparata, in *Lepton and Hadron Structure,* proceedings of the 1974 International School of Subnuclear Physics, Erice, Italy, edited by A. Zichichi (Academic, New York, 1975), p. 54.
[13]G. Preparata and N. Craigie, Nucl. Phys. B102, 478 (1976).
[14]G. Preparata and K. Szego, Phys. Lett. 68B, 239 (1977); Nuovo Cimento 47A, 303 (1978).
[15]G. Preparata, Nucl. Phys. B122, 29 (1977).
[16]C. Bourrely, E. Leader, and J. Soffer, Phys. Rep. 59, 95 (1980).
[17]*Elastic and Charge Exchange Scattering of Elementary Particles,* Vol. 7 of *Landolt-Bornstein, New Series,* edited by H. Schopper (Springer, Berlin, 1973).
[18]R. Blankenbecler, S. J. Brodsky, and J. F. Gunion, Phys. Rev. D 8, 287 (1973).
[19]B. Pire, Nucl. Phys. B114, 11 (1976).
[20]R. Almas *et al.*, Phys. Lett. 93B, 199 (1980).
[21]C. Baglin *et al.*, Nucl. Phys. B98, 365 (1975).
[22]J. Chauveau, thesis, Université Pierre et Marie Curie, Paris, 1981 (unpublished).
[23]S. J. Brodsky and G. R. Farrar, Phys. Rev. Lett. 31, 1153 (1973); V. Matveev, R. Muradyan, and A. Tavkhelidge, Lett. Nuovo Cimento 7, 779 (1973).
[24]S. Brodsky and G. Lepage, Phys. Rev. D 22, 2157 (1980).
[25]P. V. Landshoff, Phys. Rev. D 10, 1024 (1974).
[26]A. Mueller, Phys. Rep. 73C, 237 (1981); P. Landshoff and D. Pritchard, Z. Phys. C 6, 69 (1980).
[27]J. Ralston and B. Pire, Phys. Lett. 117B, 233 (1982).
[28]A. Yokosawa, in *High Energy Physics with Polarized Beams and Polarized Targets,* proceedings of the 1980 International Symposium, Lausanne, Switzerland, edited by C. Joseph and J. Soffer (Birkhauser, Basel, Switzerland and Boston, 1981), Exp. Suppl. Vol. 38, p. 261.
[29]P. Chiappetta and J. Soffer, in *High Energy Spin Physics—1982,* proceedings of the 5th International Symposium, Brookhaven National Laboratory, edited by G. Bunce (AIP, New York, 1983), p. 352.